Feedstock material property – process relationships in fused deposition of ceramics (FDC)

N. Venkataraman, S. Rangarajan, M.J. Matthewson, B. Harper, A. Safari, S.C. Danforth, G. Wu, N. Langrana, S. Guceri and A. Yardimci

The authors

N. Venkataraman, S. Rangarajan, M.J. Matthewson, B. Harper, A. Safari and **S.C. Danforth** are at the Department of Ceramic and Materials Engineering, Rutgers University, Piscataway, New Jersey, USA.
G. Wu and **N. Langrana** are at the Department of Mechanical & Aerospace Engineering, Rutgers University, Piscataway, New Jersey, USA.
S. Guceri is at the Department of Mechanical Engineering, University of Illinois at Chicago, Illinois, USA.
A. Yardimci is at the Advanced Engineering Design Center, Baxter International, Illinois, USA.

Keywords

Solid freeform fabrication, Deposition, Rheology, Ceramics

Abstract

Fused deposition of ceramics (FDC) is a solid freeform fabrication technique based on extrusion of highly loaded polymer systems. The process utilizes particle loaded thermoplastic binder feedstock in the form of a filament. The filament acts as both the piston driving the extrusion and also the feedstock being deposited. Filaments can fail during FDC via buckling, when the extrusion pressure needed is higher than the critical buckling load that the filament can support. Compressive elastic modulus determines the load carrying ability of the filament and the viscosity determines the resistance to extrusion (or extrusion pressure). A methodology for characterizing the compressive mechanical properties of FDC filament feedstocks has been developed. It was found that feedstock materials with a ratio (E/η_a) greater than a critical value (3×10^5 to 5×10^5 s^{-1}) do not buckle during FDC while those with a ratio less than this range buckle.

Electronic access

The research register for this journal is available at **http://www.mcbup.com/research_registers/aa.asp**

The current issue and full text archive of this journal is available at **http://www.emerald-library.com**

Rapid Prototyping Journal
Volume 6 · Number 4 · 2000 · pp. 244–252
 · ISSN 1355-2546

Introduction

Fused deposition of ceramics (FDC) is a solid freeform fabrication technique based on fused deposition modelling (FDM^{TM}) and involves extrusion of highly loaded polymer systems. The FDC process is currently being used to fabricate functional components of a variety of ceramic and metallic materials such as: Si_3N_4, lead zirconate titanate (PZT), Al_2O_3, hydroxyapatite and stainless steel for a variety of structural, electroceramic and bioceramic applications (Agarwala *et al.*, 1996a; Bandyopadhyay *et al.*, 1997; Danforth *et al.*, 1998; Safari *et al.*, 1998). The FDC process utilizes particle loaded thermoplastic binder feedstock in the form of a 1.78 ± 0.025mm diameter filament. The filament is fed via a pair of counter-rotating rollers into a heated liquefier, Figure 1. The molten feedstock is then deposited in the X-Y plane onto a Z stage platform to fabricate the green part. The filament acts as both the piston driving the extrusion process and the feedstock of the material being deposited. The most common mode of failure of the filament feedstock in the FDC process is "buckling" (Figure 1). The pressure drop, ΔP, needed to extrude material through the FDC nozzle depends on the viscosity of the feedstock, the nozzle geometry, the orifice size and the volumetric flow rate (Rangarajan *et al.*, 1999; Benbow *et al.*, 1993; Zheng *et al.*, 1992). Since the exit pressure is nearly atmospheric, ΔP can be assumed to be the relevant pressure on the filament, when described in absolute pressure terms. If this pressure exceeds the critical load per unit area for the filament, buckling ensues and the process is interrupted.

The buckling criterion for elastic columns is given by Euler's analysis for pin ended boundary condition as (Beer and Johnston, 1992):

This work was sponsored by the Office of Naval Research under ONR MURI contract number N00014-96-1-1175. The authors also acknowledge the significant assistance provided by Thomas McNulty, Farhad Mohammadi, Eric Passman, Rhea Jaico, Brian Harper, Gouhua Wu and Ewan Bossett in this work. The miniature materials tester was obtained with financial support of Allied Signal under DARPA/ONR contract No. N00014-94-C-0115.

Figure 1 Schematic of the FDC liquefier showing the important process and material parameters involved in buckling

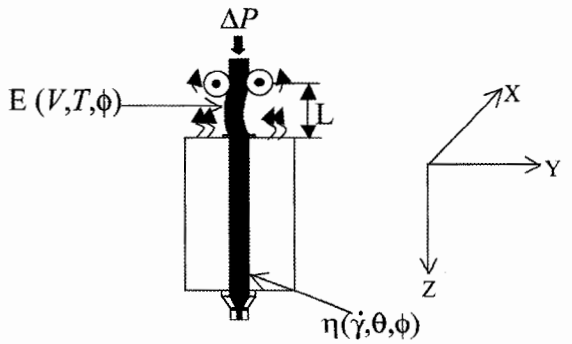

ΔP: Extrusion Pressure, V: Filament feed rate, T, θ: temperature, ϕ: solids loading, $\dot{\gamma}$: shear rate, η: viscosity of feedstock, E: compressive stiffness of filament

$$\sigma_{cr} = \frac{\pi^2 E}{4(L/R)^2} \quad (1)$$

where: σ_{cr} is the critical buckling stress, E is the elastic modulus (compressive modulus for FDC filaments), L is the length of the column (in this case, the length of the filament between the rollers and the top of the liquefier), R is the radius of the filament.

The pressure drop (ΔP) in a capillary rheometer required to drive a non-Newtonian fluid through a tube of length l and radius r is given by (van Vazer, 1963; Barnes *et al.*, 1996):

$$\Delta P = \frac{8\eta_a Q l}{\pi r^4} \quad (2)$$

where: η_a is the apparent viscosity determined using a capillary rheometer, Q is the volumetric flow rate. The FDC process involves the extrusion of a shear thinning material through a straight tube section (the liquefier) and a nozzle. In a capillary rheometer, the material flows through a barrel and a capillary and therefore closely approximates the flow behavior in the FDC process. As a result one can make the following assumption. If a particular material needs a higher pressure for extrusion in the capillary rheometer than another material does (for a fixed capillary and volumetric flow rate); it will also require a correspondingly higher extrusion pressure in the FDC process (for a fixed nozzle/liquefier geometry and volumetric flow rate).

Let us consider two materials A and B. Let their capillary extrusion pressure measured using a particular capillary and at a given volumetric flow rate be, ΔP_A and ΔP_B respectively. Now let us consider that one wishes to compare their (i.e. A and B) buckling behavior in the FDC process for a particular nozzle and volumetric flow rate. Let their corresponding FDC extrusion pressures be, $\Delta P'_A$ and $\Delta P'_B$ respectively. Then the assumption made in this study suggests that if $\Delta P_A > \Delta P_B$, then $\Delta P'_A > \Delta P'_B$. Also, it is known that if $\Delta P_A > \Delta P_B$ for a given capillary and volumetric flow rate, then the corresponding apparent viscosity of A is also higher than that of B (equation (2)). If one assumes then that there is a scaling factor, k between the capillary extrusion pressure and FDC extrusion pressure for any material, one can then say that $\Delta P = k\,\Delta P'$. Also, filaments in FDC will buckle when the FDC extrusion pressure exceeds the critical buckling stress:

$$\text{i.e. } \Delta P' > \sigma_{cr} \text{ or } \Delta P/k > \sigma_{cr}, \quad (3)$$

where: ΔP and $\Delta P'$ are the capillary extrusion pressure and FDC extrusion pressure of a particular material, respectively. From equations (1), (2) and (3) one can write that FDC filaments will buckle if:

$$E/\eta_a < \frac{8Ql(L/R)^2}{\pi^3 r^4 k} \quad (4)$$

Therefore, one can see from equation (4) that if E/η_a of a material exceeds a critical value it will buckle. Now the critical value as shown in equation (4) will depend on the volumetric flow rate, Q (in the capillary rheometer), the capillary (length, l and radius, r), the slenderness ratio of the filament (L/R in equation (1)) and the scaling factor k. In order to estimate the theoretical value of the critical value of E/η_a one will need to estimate the value of the scaling factor k.

The factor k, is the scaling factor between the capillary extrusion pressure and the FDC extrusion pressure for a particular filament material. It can possibly depend on the particular capillary/FDC nozzle combination used, the material being used in capillary extrusion or FDC extrusion and the volumetric flow rates used in the capillary and FDC process. Currently, it is theoretically difficult to estimate this value of the scaling factor, k and thereby, the critical value of E/η_a.

The objective of this study is to establish the relationship between some measurable properties of the filament and the buckling behavior during FDC. This is important as it helps to understand the reasons for the

Rapid Prototyping Journal
Volume 6 · Number 4 · 2000 · 244–252

buckling of the filaments during FDC in terms of material properties. This knowledge can then guide the efforts to develop filaments for FDC by providing target values (or range of values) for some material properties (in order to prevent buckling during FDC). The FDC filament fabrication process involves a number of steps and is labor and time intensive. In addition, some of the ceramic and metallic powders could also be expensive. Therefore, the presence of scientific guidelines in the form of some target properties can help save time, labor and material costs during the development of filaments to be used in FDC.

One can see from equation (4) that for a given nozzle geometry, capillary geometry, liquefier design, roller design, filament dimensions and flow rate, filaments with a value of E/η_a greater than a critical value will work in FDC without buckling. Therefore, filaments need to have greater than some critical value of E/η_a to prevent failure via buckling (where, η_a is the apparent viscosity of the material at the FDC temperature measured using a particular capillary and is a function of shear rate). The E/η_a ratio also determines the window of operation for the FDC process (in terms of possible solids loading, liquefier temperature and volumetric flow rates). The filament feedstock mechanical and rheological properties therefore, can be used to define FDC process limits from a materials perspective.

This paper discusses the methodology developed for characterization of the compressive modulus and viscosity of FDC materials. The E/η_a ratio for various feedstock materials was determined. Based on the E/η_a ratio, a materials selection map has been developed. The use and limitations of this materials selection map will also be discussed.

Experimental procedure

A list of the different feedstock materials evaluated is given in Table I. The different binders used for fabrication of the feedstock are designated RU9, ECG9 and ECG2. The details of the binder compositions and binder development have been presented elsewhere (McNulty *et al.*, 1998; Agarwala *et al.*, 1996b). The binders are all multicomponent and consisting primarily of thermoplastics. The different powders used are PZT, Si_3N_4, graphite and 17-4PH stainless steel powder (spherical and irregular) (Wu *et al.*, 1999). The particle size, density and surface area of each powder are presented in Table II. The dispersants used were oleyl alcohol (Fisher Scientific) for Si_3N_4 and stearic acid (Fisher Scientific) for all other powders (McNulty *et al.*, 1999).

The detailed procedure for coating Si_3N_4 with oleyl alcohol is presented elsewhere (Rangarajan *et al.*, 1999). The PZT, graphite, powders were coated with stearic acid (Table I) in a Nalgene™ bottle for four hours in a ball mill. A ZrO_2 mixing medium (9.525mm, cylindrical) was used. The slurry obtained at the end of the mixing step was then vacuum filtered. The resulting powder cake was dried for 12 hours, followed by compounding with the appropriate binder in a torque rheometer (Haake). The details of the compounding procedure for PZTECG9 and RU955 are presented elsewhere (Rangarajan *et al.*, 1999; Venkataraman *et al.*, 1999). GRECG9, GRECG9SA were compounded according to the conditions presented in Table I.

The compounded material of each feedstock was granulated. The granulated material was used directly for capillary rheology measurements. The granules were stored in a dessicator prior to the testing. PZTECG9 and RU955 filaments were fabricated via single screw extrusion. The GRECG9 series, GRRU9 series filaments were fabricated via piston extrusion. In the screw extrusion step, the granules were fed via a hopper into a screw extruder (Haake). The pressure and temperature in three zones of the screw extruder were monitored and controlled. A 120 mesh screen and breaker plate arrangement was used to remove agglomerates and also to obtain homogeneous mixing during screw extrusion. A 1.78mm extrusion diameter nozzle was used. The extruded filaments were picked up by a conveyor belt whose speed was matched to the extrusion speed to control the diameter of the filament to 1.778mm ± 0.025mm. The filaments were spooled and stored in a controlled humidity environment (25 per cent RH) until further use. In piston extrusion, a heated barrel was filled with granules. A precision-machined capillary nozzle of 1.78mm was attached to one end of the heated barrel. The barrel was moved in a controlled fashion (1mm/min linear velocity)

Table I Feedstock materials used for FDC and E/η_a analysis

Material designation	Ceramic/metal (Vol. %)	Binder	Compounding temperature (°C)	Sufactant (wt % based on powder)
PZTECG9	PZT[a] (52.6)	ECG9	160	Stearic acid (3%)
RU955	Si3N4[b](55)	RU9	100	Oleyl alcohol (3%)
GRRU9	Graphite[c] (55)	RU9	100	None
GRRU9OA	Graphite[c] (55)	RU9 + 3wt.% Oleyl alcohol	100	None
GRECG9	Graphite[c] (55)	ECG9	140	None
GRECG9SA	Graphite[c] (55)	ECG9	140	Stearic acid (3%)
17-4PHECG2sph	17-4PH[d] (58) Spherical powder	ECG2	165	Stearic acid (1%)
17-4PHECG2Irr	17-4 PH[e] (58) Irregular powder	ECG2	165	Stearic acid (1%)
ICW06	Neat wax (0)	ICW06	Not applicable	Not applicable

Notes: [a]TRS, Inc., University Park, PA. [b]Supplied by Allied Signal, CA. [c] Source, Alfa Aesar. [d] Source Anval, Inc. [e] Source, Ametek, Inc.

Table II Powder characteristics

Powder	Average particle Size (μm)	Density (g/cm^3)	Surface area (m^2/g)
Silicon nitride	0.395	3.2	7.31
PZT	0.73	7.96	2.58
Graphite	22	2.2	5.6
17-4PH spherical	17	7.8	0.05[a]
17-4PH irregular	22	7.8	0.035[a]

Note: [a]Calculated surface area using equivalent spherical radius

onto a precision-machined plunger. The filaments were extruded through the capillary nozzle and were cut at regular intervals. The filaments obtained in this fashion were also stored in a controlled humidity environment (25 per cent RH). The coating and fabrication procedure of the 17-4PHECG2 series filaments have been reported elsewhere (Wu *et al.*, 1999). In addition to the particle loaded systems a commercial unfilled material designated ICW06 (Stratasys, Inc., Eden Prairie, Minnesota) (investment casting wax) was also characterized.

Mechanical characterization

Filaments of all of the feedstock materials were tested in compression using a miniature materials tester (Rheometrics Scientific, Inc.), Figure 2. The aspect ratio (L/D) of the filament samples used for compression testing was 1.5 (Odom and Adams, 1994). All samples were made using a template of the required length. The end faces of the test samples were then polished using a 600 grit SiC polishing paper to achieve flat, parallel

Figure 2 Schematic of mechanical testing system showing configuration of sample and environmental chamber in the miniature materials tester

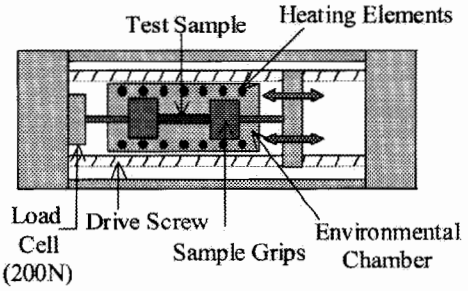

faces. Samples were stored in a controlled humidity chamber prior to testing. The frictional effects between the specimen and the grips were reduced by use of a dry lubricant.

The samples were all tested at displacement rates of 0.1, 1, 5, 10, 20mm/min. The range of displacement rates for compressive testing was chosen to encompass the possible displacement rates in the FDC process. All room temperature tests were performed on a single day to avoid perturbations due to variations in storage time and temperature. A minimum of seven samples was tested for each displacement rate. Statistically significant differences between results were ascertained using Tukey's test method.

Videomicroscopy of the tests was conducted to understand the behavior of the sample during testing. Photomicroscopy was also conducted on samples obtained from interrupted tests, to help identify the different

regions of the stress/strain behavior of the compressive test.

Rheological characterization

The viscosity of the various feedstock materials was characterized using a capillary rheometer which consisted of a 9.525mm internal diameter barrel, at the end of which was attached a capillary of a particular aspect ratio (length/diameter = 20, diameter = 1.422mm). The barrel was heated to a particular temperature, and controlled to within ±0.3°C. Granules of the compounded material were fed into the barrel. Care was taken to avoid development of any air gaps during the barrel filling step. The barrel was then moved onto the plunger until some material was extruded through the capillary. The system was held at this position for 30 minutes to allow equilibration at the end of which tests were conducted. The temperatures at which the tests were conducted were chosen as the FDC temperature for each material. RU955 was tested at 185°C, ICW06 at 70°C and all others at 140°C. The tests were run at displacement rates ranging from 2mm/min to 200mm/min, and the corresponding loads were measured via a load cell. The load cell output was then used to calculate the apparent shear stress at the wall (van Vazer, 1963; Barnes *et al.*, 1996). The volumetric flow rate was calculated from the velocity, which then yields the apparent shear rate (van Vazer, 1963; Barnes *et al.*, 1996). A minimum of three runs was performed for each material at the appropriate temperatures. The ratio of apparent shear stress to shear rate τ_a/γ_a yields the apparent viscosity, η_a, of the particular material at a given temperature.

Results and discussion

Mechanical properties

The typical normalized compressive stress strain curves for some of the feedstock materials are shown in Figure 3. It can be seen from Figure 3 that there is a non-linear region at low strain (< 8 per cent strain) which has been ascertained to be due to the load train picking up slack via independent testing with machined brass samples. At higher strains (> 8 per cent) the stress/strain behavior is roughly linear, until at even higher strains (> 15 per cent) a second region of non-linearity is observed. Videomicroscopy observations made during compression testing have established that this second non-linearity is due to some amount of barreling of the samples. Most samples exhibit a peak stress at which the sample cracks and fails. RU955 does not exhibit a peak stress at failure and the post failure stress strain behavior shows an increase in stress with strain.

Figure 3 Normalized stress (σ/σ_{max}) versus strain for FDC feedstock materials showing the stress-strain behavior typical of materials tested in compression at 25°C

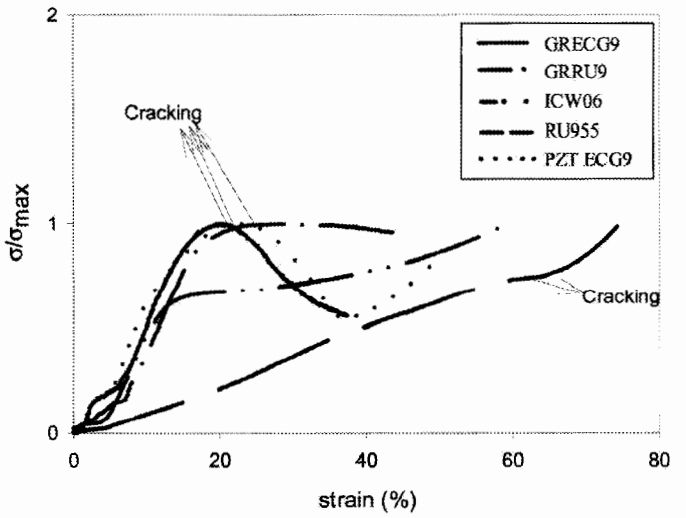

The only unfilled material tested (ICW06) exhibits a stress strain behavior as seen in Figure 3. It exhibits a linear region up to about 12 per cent strain. From 12 per cent strain to about 21 per cent strain there is a plateau region, and this is associated with yielding of the sample as observed visually. At still higher strains (>21 per cent) there is a non-linear region associated with extensive plastic deformation (the material tends to flow radially outward). The ICW06 sample does not exhibit a single peak stress at which the sample cracks, but instead tends to exhibit failure by tearing at the end of extensive plastic deformation.

The slope of the initial linear region (with a correlation coefficient greater than 0.99) is selected as the compressive modulus for each material. The compressive modulus of a few of the materials and the dependence on displacement rate is shown in Figure 4. It is found that PZTECG9, GRECG9 and GRECG9SA exhibit a modest but statistically significant increase in compressive modulus with displacement rate. In contrast none of the other materials exhibit this dependence of

Figure 4 Compressive modulus (25°C) versus displacement rate for various FDC filament materials

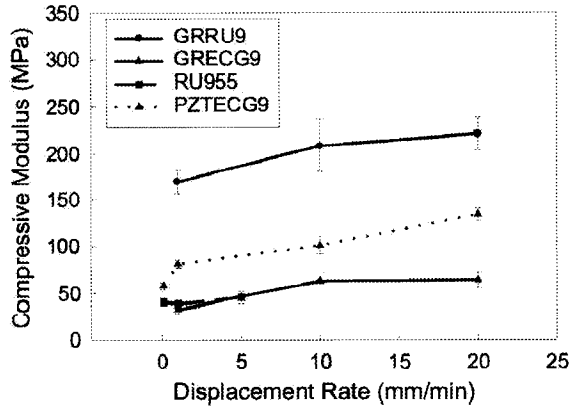

compressive modulus on displacement rate. The behavior of the mechanical properties of PZTECG9 has been discussed in more detail elsewhere (Venkataraman *et al.*, 1999). Since the modulus of the ECG9 based materials increases with displacement rate, the modulus at the lowest displacement rate of testing was chosen for use in the buckling analysis. This would correspond to the worst case scenario at the start up of the FDC process. The lowest rate used was 1mm/min. The compressive modulus of various materials was determined at room temperature (25°C) and is given in Table III. The filament above the liquefier could possibly be at a higher temperature than 25°C, but the material with a higher room temperature modulus was expected to have a higher modulus at elevated temperatures. Also, the primary purpose of this work was to compare the various materials used in FDC and therefore, the modulus at 25°C was used in all the analysis presented in this work.

As mentioned before, the compressive modulus is a crucial parameter that determines whether a filament buckles during FDC. Buckling is a failure mode commonly encountered in many structural members subjected to compressive loading. When a structure such as a rod or bar is loaded in axial compression, it can either undergo pure compressive deformation or bending. The phenomenon in which the mode of deformation abruptly changes from compression to bending is called lateral buckling (Beer and Johnston, 1992; Timoshenko and Gere, 1961). The Euler's buckling criterion can be calculated for various boundary conditions. The actual boundary condition in the FDC process could be two hinged ends, one fixed end and one hinged end or two fixed ends. As the actual boundary condition is not known exactly, the boundary condition yielding the lowest value of the buckling stress (i.e. two hinged ends) was chosen, as shown in equation (1).

Table III Measured compressive modulus of the various materials used in materials selection map

Material	Modulus (MPa)
PZTECG9	58 ± 3
RU955	41 ± 3
GRRU9	169 ± 13
GRRU9OA	94 ± 9
GRECG9	34 ± 4
GRECG9SA	45 ± 3
17-4PHECG2sph	30 ± 1
17-4PHECG2Irr	42 ± 2
ICW06	126 ± 20

The filament used in this work is a composite of ceramic/metal particles in a polymer matrix. In the literature, buckling of polymers is usually treated using Euler's criterion with the elastic modulus (in the case of elastic buckling) or tangent modulus in case of inelastic buckling (nonlinear region of the stress strain curve) (Odom and Adams, 1994; Timoshenko and Gere, 1961; de Teresa *et al.*, 1985; Rein and Cohen, 1995; Lee and Santhosh, 1993; Santhosh *et al.*, 1995; Swanson, 1992; Lankford, 1995). The magnitude of the calculated buckling stress will vary with the use of tangent or elastic modulus, but a material with a higher elastic modulus than another material can be expected to have a higher tangent modulus as well. Therefore, as the primary purpose of this work was to compare the behavior of the different FDC materials, the authors chose to use the elastic modulus instead of the tangent modulus.

The modulus, which represents the ability of a filament to withstand a certain amount of pressure without buckling has been discussed in this section. The other aspect of the buckling problem is the resistance to extrusion (or the actual pressure needed to drive the extrusion) in the FDC process. The rheological properties (viscosity) which determine the pressure needed for extrusion will be discussed now.

Rheological properties

The viscosity of the FDC feedstock materials was measured using a capillary viscometer. The capillary viscometer very closely approximates the extrusion process involved in FDC. The capillary used in this study had a length to diameter ratio of 20 and an inner diameter of 1.422mm.

The apparent viscosity versus shear rate for the different materials is plotted in Figure 5. It should be noted that the viscosity versus shear rates were measured at the FDC process temperature for each material. As seen from Figure 5, all materials show a decreasing apparent viscosity with increasing shear rate, i.e. shear thinning. Also the materials ICW06, PZTECG9, RU955, 17-4PHECG2sph and 17-4PHECG2Irr seem to be grouped together at the low viscosity region, while GRRU9, GRRU9OA, GRECG9SA and GRECG9 seem to be grouped at a higher viscosity region. This indicates that the materials containing graphite (a possible fugitive material) will exhibit a higher resistance to extrusion at the respective FDC temperatures than ICW06, RU955, PZTECG9, 17-4PHECG2sph and 17-4PHECG2Irr.

Materials selection map

In the materials selection map, Figure 6, the E/η_a for the various materials are plotted as a function of the shear rate, where η_a is measured at the liquefier temperature using a particular capillary. In Figure 6, there is a marked region (shear rates between 100 to 200s^{-1}), which indicates the typical shear rate regime for FDC through a 508μm nozzle. This region is marked because independent testing of the materials in FDC was done in this range of shear rates and all conclusions drawn with respect to FDC will relate to this nozzle size and range of shear rates. If any other nozzle size is to be used the range of shear rates will shift to the left or right depending on whether the nozzle is greater than the 508μm or smaller. Testing has shown that the following materials work in FDC without buckling: ICW06, PZTECG9, RU955, 17-4PHECG2sph and 17-4PHECG2Irr. In contrast, all GRECG9 series and GRRU9OA filaments buckle during FDC. Figure 6 shows that the materials that do not buckle lie above or near the RU955 curve in the marked region. The materials that buckle in FDC lie below the RU955 curve. This trend indicates that a critical value of E/η_a is required for FDC. Materials with values below this critical value buckle during FDC. The critical value is expected from this study to lie on or near the RU955 curve which corresponds to E/η_a in the range of 3×10^5 to $5 \times 10^5 s^{-1}$.

It was discussed in the introduction that the critical value of E/η_a, depends on volumetric flow rate, Q (in the capillary rheometer), the capillary (length, l and radius, r), the slenderness ratio of the filament (L/R in equation (1)) and the scaling factor k. Also, the scaling factor k, between the capillary extrusion and FDC extrusion pressure for a material can possibly depend on the particular capillary/nozzle combination used, the

Figure 5 Apparent viscosity vs shear rate for various FDC feedstock materials tested in the capillary rheometer at the liquefier temperature

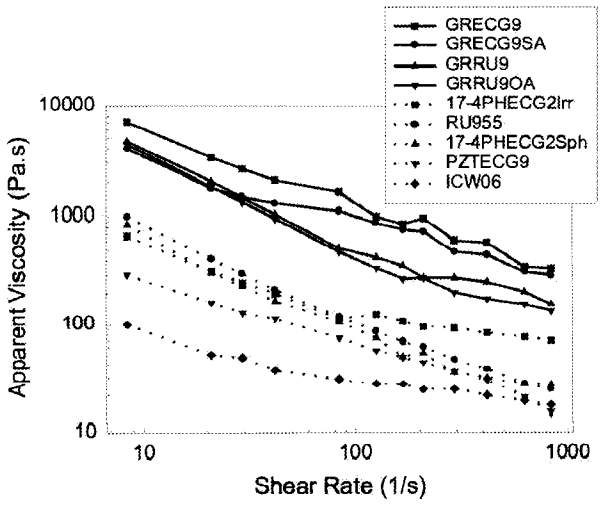

Figure 6 A materials selection map for FDC feedstock materials showing the ratio of E/η_a plotted as a function of shear rate. The materials that lie above or near RU955 do not buckle in FDC. In contrast the materials that have E/η_a below RU955 buckle in FDC

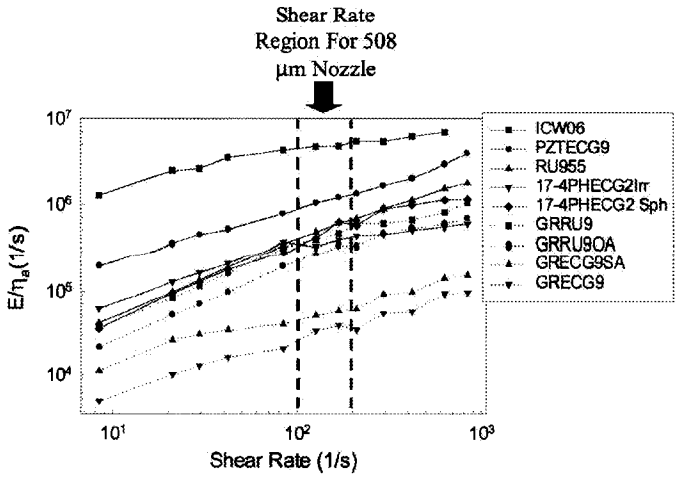

material being used in capillary extrusion or FDC extrusion and the volumetric flow rates used in the capillary and FDC process. In our study the comparison of the different materials was done at a particular shear rate (or over a range of shear rates), for a given capillary/nozzle combination. This therefore, fixes the capillary/nozzle combination (and thereby the capillary geometry and FDC nozzle geometry as well) and the volumetric flow rates (in FDC and capillary) over which all the materials were being compared. The present study suggests that for the materials studied so far in this study, the critical value of E/η_a, is around 3×10^5 to 5×10^5 over the shear rate range of 100 to 200s^{-1} used. Therefore, the critical value increases as one increases the shear rate, but is pretty much a unique value for a given shear rate. Therefore, one can conclude that the value of the scaling factor k, does not show a variation with the materials considered in the present study. If the value of k depends on the particular material considered then one will find that there will be a range of critical values for the modulus to viscosity ratio (depending on the material being considered) at a given shear rate (keeping all other conditions the same as mentioned earlier).

The map developed in this work is to be used for materials selection purposes only. The map does not indicate the process performance in terms of the various process parameters such as temperature, nozzle geometry, and other design parameters. The attempt is to show that the ratio of the compressive modulus to apparent viscosity measured under standard conditions can be used to predict which material will be successful in FDC without buckling.

The FDC process has "start up" regions during which the liquefier pumping mechanism accelerates to a steady state value. Within these regions the materials typically experience a transient state of stress. The materials used in the extrusion process are all filled thermoplastics and therefore, exhibit rate dependent rheological and mechanical behavior (Aklionis and MacKnight, 1983). The use of steady state properties such as compressive modulus (at one rate) and steady state viscosity values (at an average steady state shear rate) to predict a transient process such as FDC (for materials that exhibit rate and history dependent behavior) may contribute to some limitations in the use of E/η_a to predict the buckling behavior of FDC filaments. Therefore, in the future, the dynamic mechanical and rheological behavior of the materials should be characterized and used to predict the materials' behavior in FDC.

The present analysis establishes that a critical ratio of E/η_a exists for the filaments to function without buckling in FDC and establishes that the material development efforts should take care of this balance of stiffness and viscosity to avoid buckling in FDC.

Summary and conclusions

A methodology for characterizing the compressive mechanical properties of FDC filament feedstock materials was developed. The compressive modulus of some of the feedstock materials exhibits a significant rate dependence, i.e. the modulus increases with increasing rates, while others do not. The apparent viscosity of the feedstock materials was characterized at the appropriate temperature (the respective FDC temperature) via capillary rheometry. All the feedstock materials exhibit a shear thinning behavior in the range of shear rates studied. The ratio of the compressive modulus to the apparent viscosity (measured at a particular temperature using a particular capillary), E/η_a, was shown to represent the ability of the material to function in FDC without buckling. A materials selection map based on E/η_a was developed in this work. It was found from this study that the FDC feedstock materials do exhibit a critical E/η_a ratio, which was found to be in the range of 3×10^5 to $5 \times 10^5 s^{-1}$. Filaments with a ratio above the critical limit do not buckle in FDC. The map does not indicate the process performance in terms of the various process parameters such as temperature, nozzle geometry, and other design parameters. The attempt is to show that the ratio of the compressive modulus to apparent viscosity measured under standard conditions can be used to predict which material will work in FDC without buckling. It has been established that a balance of the properties such as stiffness and viscosity is necessary for the successful functioning of FDC filament feedstock material.

References

Agarwala, M.K., Bandyopadhyay, A., van Weeren, R., Safari, A. and Danforth, S.C. (1996a), "FDC, rapid fabrication of structural components (fused deposition of ceramics)", *American Ceramic Society Bulletin*, Vol. 75 No. 11, pp. 60-65.

Agarwala, M., Danforth, S.C., van Weeren, R., Bandyopadhyay, A., Safari, A. and Priedeman, W. (1996b), "Filament feed materials for fused deposition processing of ceramic and metals", in Bourell, D.L., Beamen, J.J., Marcus, H.L., Crawford, R.H. and Barlow, J.W. (Eds), *SFF Proceedings*, Vol. 7, Austin, TX.

Aklionis, J.J. and MacKnight, W.J. (1983), *Introduction to Polymer Viscoelasticity*, 2nd ed., John Wiley and Sons, New York, NY.

Bandyopadhyay, A., Panda, R.K., Janas, V.F., Danforth, S.C. and Safari, A. (1997), "Processing of piezocomposites by fused deposition technique", *Journal of the American Ceramic Society*, Vol. 80 No. 6, pp. 1366-72.

Barnes, H.A., Hutton, J.F. and Walters, K. (1996), *An Introduction to Rheology*, Elsevier, Amsterdam.

Beer, F.P. and Johnston, E.R. (1992), *Mechanics of Materials*, 2nd ed., McGraw-Hill, London.

Benbow, J. and Bridgwater, J. (1993), *Paste Flow and Extrusion*, Crookall, J.R., Shaw, M.C. and Suh, N.P. (Eds), Clarendon Press, Oxford.

Danforth, S.C., Agarwala, M.K., Bandhyopadhyay, A., Langrana, N., Jamalabad, V.R., van Weeren, R. and Safari, A. (1998), "Solid freeform fabrication methods", US Patent No. 5738817.

de Teresa, S.J., Porter, R.S. and Farris, R.J. (1985), *Journal of Materials Science*, Vol. 20, pp. 1645-59.

Lankford, J. (1995), "Compressive failure of fibre-reinforced composites: buckling, kinking and the role of the interphase", *Journal of Materials Science*, Vol. 30, pp. 4343-8.

Lee, C.Y-C. and Santhosh, U. (1993), "The role of the fibrillar structures in the compressive behavior of rigid-rod polymer fibers", *Polymer Engineering and Science*, Vol. 33 No. 14, pp. 907-12.

McNulty, T., Shanefield, D.J., Danforth, S.C. and Safari, A. (1999), "Dispersion of lead zirconate titanate for fused deposition of ceramics", *Journal of the American Ceramic Society*, accepted for publication.

McNulty, T., Mohammadi, F., Bandyopadhyay, A., Shanefield, D.J., Danforth, S.C. and Safari, A. (1998), "Development of a binder formulation for fused deposition of ceramics", *Rapid Prototyping Journal*, Vol. 4 No. 4, pp. 144-50.

Odom, E.M. and Adams, D.F. (1994), "Development of an improved compression specimen geometry for unreinforced polymers", *Journal of Testing and Evaluation*, pp. 104-10.

Rangarajan, S., Qi, G., Venkataraman, N., Safari, A. and Danforth, S.C. (1999), "Powder processing, rheology and mechanical properties of feedstock for fused deposition of Si_3N_4 ceramics", submitted to *Journal of American Ceramic Society*.

Rein, D.M. and Cohen, Y. (1995), "Mechanical stability of rigid rod polymer fibres under the influence of compression and temperature", *Journal of Materials Science*, Vol. 30, pp. 3587-90.

Safari, A., Janas, V.F., Bandhyopadhyay, A., Panda, R.K., Agarwala, M., Danforth, S.C. (1998), "Ceramic composites and methods for producing same", US Patent No. 5818149.

Santhosh, U., Newman, K.E., Lee, C.Y-C. (1995), "Compressive strength of coated rigid-rod polymer fibres", *Journal of Materials Science*, Vol. 30, pp. 1895-901.

Swanson, S.R. (1992), "A micro-mechanics model for in-situ compression strength of fiber composite laminates", *Journal of Engg Materials and Technology*, Vol. 114, pp. 8-12.

Timoshenko, S.P. and Gere, J.M. (1961), *Theory of Elastic Stability*, 2nd ed., McGraw-Hill Book Company, London.

van Vazer, J.R. (1963), *Viscosity and Flow Measurement; A Laboratory Handbook of Rheology*, Interscience Publishers, New York, NY.

Venkataraman, N., McNulty, T., Rangarajan, S., Vidaic, M., Matthewson, M.J., Langrana, N., Safari, A. and Danforth, S.C. (1999), "Mechanical properties of feedstock material for fused deposition of ceramics", *Proceedings of SFF Symposium, MRS Meeting*, Vol. 542, pp. 111-17.

Wu, G., Langrana, N., Rangarajan, S., McCuiston, R., Sadanji, R., Danforth. S. and Safari, A. (1999), "Fabrication of metal components by FDMet-fused deposition of metals", in Bourell, D.L., Beamen, J.J., Marcus, H.L., Crawford, R.H. and Barlow, J.W. (Eds), *SFF Proceedings*, Vol. 10, Austin, TX.

Zheng, J., Carlson, W.B. and Reed, J.S. (1992), "Flow mechanics on extrusion through a square-entry die", *Journal of the American Ceramic Society*, Vol. 75 No. 11, pp. 3011-6.